

Fracture energy of high performance mortar subjected to high temperature

S. Djaknoun & E. Ouedraogo

Domaine Universitaire, BP 53, 38041 Grenoble CEDEX 09, France.

A. Ahmed Benyahia

Laboratoire de Mécanique Avancée (LMA), FGM&GP de L'USTHB, BP 32 El-Alia, 1611 Alger, Algeria.

ABSTRACT: A three-point bending test apparatus for testing concrete-like materials at high temperatures has been developed. Notched specimens were heated at a rate of 3.3°C per minute to various temperatures, up to a maximum of 900°C . They were then subjected to a three-point bending test while the temperature was held constant. The maximum peak load occurred in the temperature range of 300 to 500°C , and decreased sharply at higher temperatures. The experimental results demonstrated a noticeable nonlinear effect of the temperature on the fracture resistance of mortar for high performance concrete. Tenacity parameters such as the stress intensity factor or the fracture energy were found to evolve with testing temperature. Temperatures in the range of 300 to 500°C led to optimal values for these parameters, whereas at higher temperatures, the parameter values decreased considerably. SEM micrographs of the heated specimens after mechanical tests facilitated the understanding of the macroscopic behaviour.

1 INTRODUCTION

Concrete is a heterogeneous material with quasi-fragile behaviour. The micro-cracking process can alter the mechanical properties of concrete. Stress-deformation curves in concrete initially undergo a linear elastic evolution and then a nonlinear evolution up to the stress peak, followed by a more or less severe softening phase. The coalescence of micro-cracks leads to the appearance of a fracture macro-crack. In many cases, this fracture is not only due to the crack propagation mechanism. Micro-cracking can be divided into two phases; the first phase begins with crack propagation throughout the initiated micro-cracks. The second phase is the subject of fracture mechanics. For concrete materials, micro-cracks are constitutive of the material, i.e., they exist prior to the application of a mechanical load. These consubstantial micro-cracks can potentially or essentially contribute to macro-crack formation leading to material failure.

The theory of elastic linear fracture mechanics is currently used to analyze metallic materials failure. All of the damage phenomena are assumed to occur at the tip of the crack. Conversely, nonlinear fracture mechanics assumes the existence of a fracture process zone (FPZ), a plane zone where damage mechanisms occur. This last approach appears to be more relevant to the analysis of isotropic materials with quasi-brittle behaviour, such as concrete, in

which the mode I fracture is dominant. Similar to nonlinear fracture mechanics, damage mechanics has been developed to model the fracture of materials while exhibiting softening behaviour; thus, it is relevant to the modelling of the crack initiation phase.

Many studies have reported an influence of mortar or concrete composition on its resistance to crack propagation (Kaplan 1961, Gjorv et al. 1977), but the results have been contradictory. Moreover, a wide variety of test temperature ranges, experimental conditions, materials composition, and cure conditions makes it very difficult to compare these published studies.

The experimental determination of crack propagation resistance within hydraulic binder materials has been widely reported, with main contributions by Swamy (1979) and Ziegeldorf (1983). Among the tests, three-point bending tests on notched specimens, defined by RILEM recommendations (RILEM 1985, RILEM 2000), are used to characterise mortar or concrete resistance to propagation, by determining the fracture energy in a mode I fracture. This method, developed by Hillerborg & Petersson (1980), performs a stable process bending test on a notched specimen. In the bending test, the stress field is nonuniform with a continuously evolving gradient along the path of crack propagation. This may result in a variation in the energy per unit area necessary for the crack to

propagate as far as the resistant section as the notch plane evolves. Moreover, in bending tests, the length of the crack propagation is relatively short, and the notch which initiates the crack propagation does not have real crack characteristics. Consequently, more energy is needed in the crack initiation process. A precise analysis of the crack propagation mechanisms shows that the fracture energy determination is affected by parasitic phenomena when the crack propagation path is short, for example if there is a high ratio of notch length to side length.

Most of the results reported in the literature report on the material behaviour at room temperature, after the concrete has been heated to various temperatures and then cooled. These studies essentially evaluate the residual resistance of the concrete materials (Diedericks et al. 1988, RILEM 2000, Felecetti et al. 1996, Schrefler 1995, Chan et al. 2000-1, Chan et al. 2000-2, Menou et al. 2006). Other more ambitious projects have tried to determine the concrete behaviour at high temperature, but these tests are more difficult to perform. In general, testing temperatures have been limited to 600°C, which is the reference temperature for fire conditions in a building. Bazant & Kazemi (1990), Khoury et al. (1985), Noumowé et al. (1994), and Felecetti et al. (1996) reported on compression or three-point bending tests, with results up to 600°C.

Most reported tests have been performed on ordinary concrete, with very few using high-performance concrete (HPC). The present study investigates HPC. Three-point bending tests have been carried out at high temperatures up to 900°C on notched specimens of HPC mortar. The evolution of the tenacity parameters with temperature have been determined and reported. Analysis of SEM micrographs of the specimens after heating and cooling has been used to help understand the material behaviour.

2 MATERIALS AND METHODS

The investigated mortar material is a mixture of calibrated normalized sand, cement, water mixed with super-plasticizer, and fine particles of fume silica. The maximum particle size of the calibrated sand is 2 mm. The cement is a CEM 52.5 product produced by Vicat, and the super-plasticizer containing polycarboxilate delivered in liquid form is from Sika. This mortar material has a low porosity, with a w/c ratio of 0.25. The mortar is placed into a mould which is vibrated according to a strict protocol. At the mid-length of the mould there are 0.1 mm width blades which form the notch during the moulding process. Then, for 24 hours the mould is protected with a plastic sheet to prevent

moisture lost. The mould produces three specimens that are calibrated in size and weight. The specimens are prismatic with a square section, and they measure 160x25x25 mm³. Although we have produced specimens with varying notch lengths, we present test results only for those that are 10 mm long. The tests were carried out on a ZWICK Z400 testing machine equipped with a 1600°C temperature heating capacity industrial furnace. The setup is equipped with a special extensometer, based on measurements of two LVDT sensors placed outside the furnace. A differential system, using alumina rods positioned axially through the furnace, measures the displacement from the upper punch toward the lower punch; this displacement theoretically corresponds to the specimen height variation in a uniaxial compression test. The high temperature three-point bending test apparatus has been adapted to this extensometer. The measured force and the displacement of the loading point are recorded during tests.

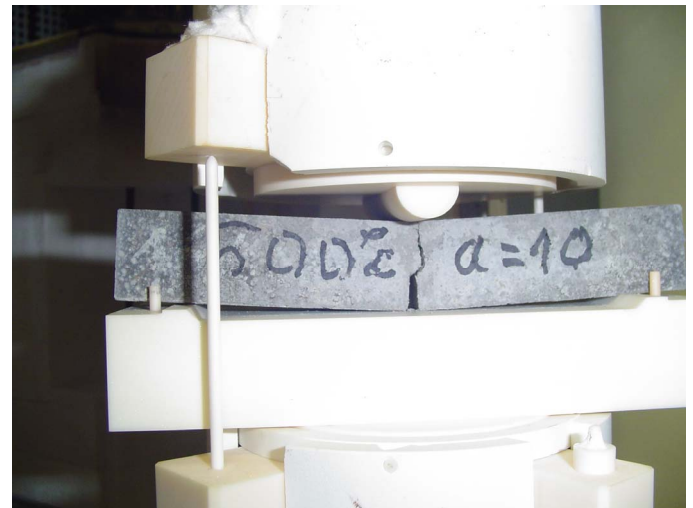


Figure 1. View of a specimen in the testing apparatus after a test is performed at 500°C temperature.

The present study specifically examines the mechanical loading while the specimen is heated. A three phase thermal cycle is applied to the material during a test: (1) a heating phase at a rate of 3.3°C/min, (2) a holding time after the target temperature is reached, and (3) a cooling phase at a rate of 2.5 °C/min. The holding time is divided into two periods. The first two-hour period is applied in all tests and is used to equalize the temperature of the specimen and the loading apparatus. The second holding time period is characterized by mechanical loading, and ends generally with the failure of the specimen; the time is variable and depends on the testing temperature. A constant 0.015 mm/min displacement rate is applied to the specimen, and the reaction force is measured during the mechanical loading. The following testing temperatures were applied: 25, 150, 300, 500, and 700°C. The material

was not tested at 900°C because its strength was insufficient. Once the specimen temperature had decreased to room temperature, it was removed from the furnace and a SEM microscopy analysis was performed.

3 RESULTS AND DISCUSSION

The applied method requires the use of deflection control for the specimen, both for measuring the dissipated energy during the complete and stable rupture of the material, and for studying the fractured section afterwards. To ensure that the crack propagation is stable with no dissipation of supplementary energy, our test imposed a displacement instead of force.

Important results were obtained on the fracture load at various temperatures using three-point bending tests. Figure 2 shows load-displacement curves from these tests performed on 10 mm notch length specimens at various testing temperatures. These results show the classical bell-shape evolution characterized by a peak load followed by a softening of the curve.

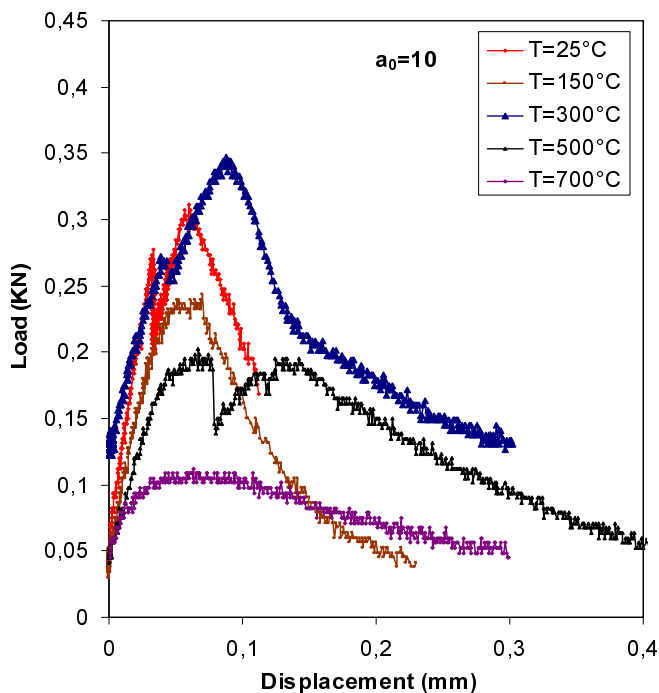


Figure 2. Evolution of the specimen maximal applied load vs. deflection, for a 10 mm length notched specimen at various testing temperatures.

A global analysis of the results suggests that the curves can be classified into two groups. The first group includes tests performed at temperatures ranging from 25 to 500°C, and are characterized by high maximal load and pronounced peaks. The second group only includes the test performed at 700°C, and is characterized by a noticeably reduced peak load followed by a progressive evolution of the

resulting load. In this case, the cracking that occurred after the load peak is more progressive and is similar to pseudo-ductility. Figure 2 shows the transition in the material behaviour as the temperature increases from 500 to 700°C. Within the first group, the peak load increases as the temperature increases from 25 to 300°C (with the exception of a slight decrease at 150°C), then the peak load decreases at 500°C.

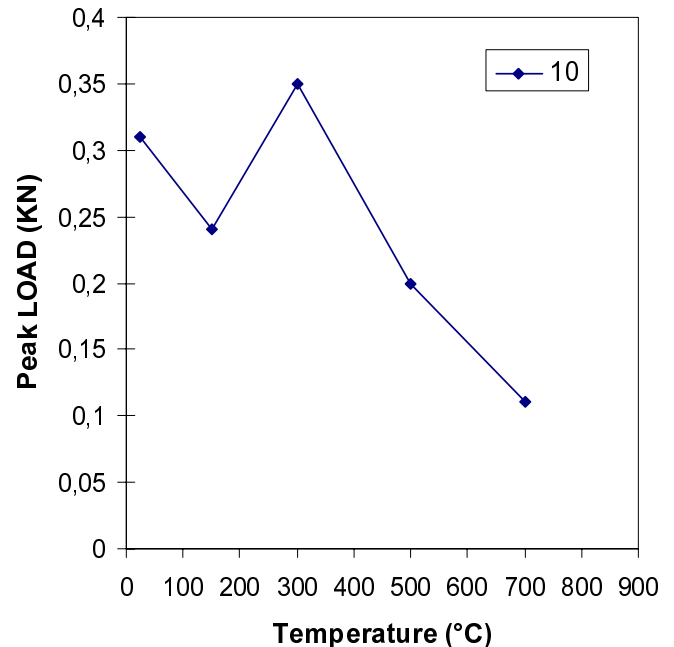


Figure 3. Variation of the maximal applied force on a 10 mm length notched specimen vs. testing temperature.

The softening of the curve during the tests at 25 and 150°C are more pronounced than at the other temperatures; this indicates that the material is more fragile at this temperature range, particularly at 150°C. In summary, the material behaviour changes notably from 500 to 700°C. Figure 3 shows the evolution of the maximal load with the testing temperatures used in Figure 2; the load values are averaged over three tests at each temperature. The decrease of the maximal load at a test temperature of 150°C is apparent. Various explanations for this phenomenon have been proposed. For example, Khoury et al. (1985) suggested that at microstructure scales at this temperature, water fluidity increases, which could induce a decrease in the Van der Waal forces between the slices of calcium silicate hydrate (CSH) coat, leading to a decrease in the surface energy of the coat. We will examine this phenomenon later.

The material tenacity has been characterized as part of the material behaviour at high temperatures. The relevant parameter is the stress intensity factor (K_I), which is determined from analytical formulas based on Mechanics of Continuum Media theory and accounts for various geometries and loading conditions.

The maximal stress intensity factor for the 10 mm notch length specimens at various temperatures are provided in Figure 4. This parameter is a linear function of the maximal load within a given test; this characteristic provides commonality to their evolutions (Fig. 3). Hence, at temperatures over 300°C, the stress intensity factor decreases sharply with increasing temperature. In other words, the material fracture resistance, as characterized by its tenacity, decreases with increasing temperature. An increase in the temperature K_I from 150 to 300°C has been observed and likely represents a restart and an acceleration of the cement dehydration process at the origin of the links between the various mortar constituents (Reference).

Fracture energy is defined as the energy necessary to create a crack with a unity surface during a mode I rupture. It can be determined from RILEM (1985) recommendations through the following equation:

$$G_F = \frac{W}{2A_{lig}} \quad (1)$$

where W = energy represented by the area under the recorded load-displacement curve (assuming that all furnished energy is used to create the crack); and A_{lig} = resistant section area situated in the notch plane.

The temperature increase has an effect on the mechanical properties of concrete; this can be seen in the evolution of the fracture energy with temperature.

Figure 5 shows how the area under the load-displacement curve, representing the total energy, changes as the temperature increases, and Figure 6 shows the evolution of the fracture energy G_F with temperature. The two curves appear similar because G_F is proportional to the energy W . Figure 6 shows a decrease of G_F at 150°C, followed by an increase until 300 °C, a slight decrease from 300 to 500°C, and finally an sharp decrease at temperatures higher than 500°C. Results at 900°C are not shown; the test could not be completed because the specimen broke during heating before the mechanical load was applied. Thus, we deduce that the material resistance and the fracture energy is null at 900°C. That is consistent with the evolution of the G_F curve in Figure 6. Figures 5 and 6 suggest that a temperature of 400°C is optimal.

To better understand material behaviour at high temperatures, we performed microstructure studies. Samples of the specimens tested at the various temperatures were cooled and analyzed using SEM. Chemical analyses were also performed but are not discussed here. Figure 7(a-b) shows typical micrographs taken at 25 and 150°C, respectively, and Figure 8(a-b-c)

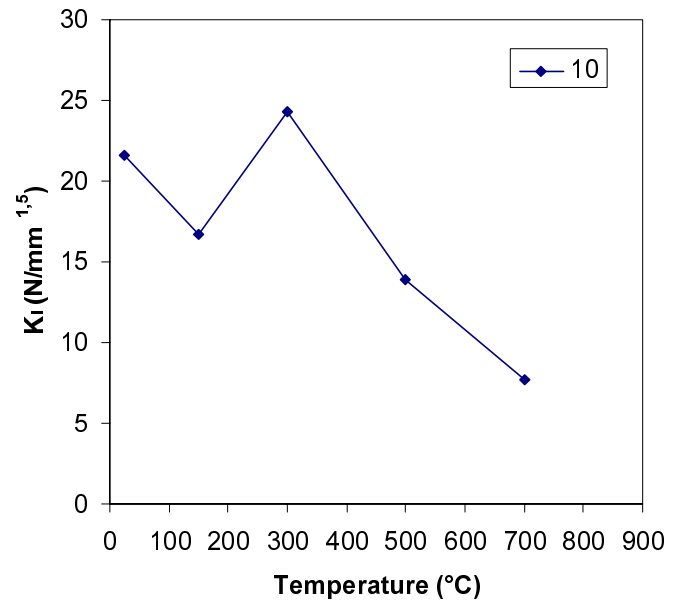


Figure 4. Evolution of the maximal stress intensity factor on the 10 mm length notched specimens vs. testing temperature.

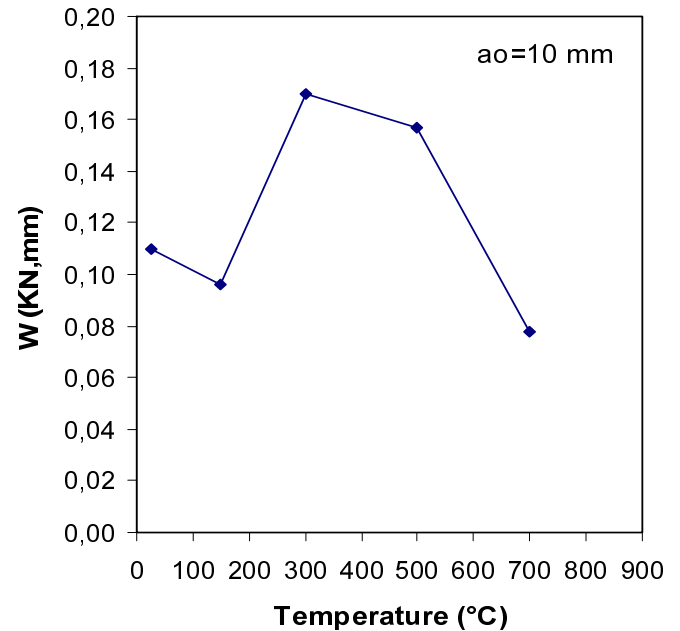


Figure 5. Evolution of the area under the load-displacement curve on the 10 mm length notched specimens vs. testing temperature.

displays those at 300, 500, and 700°C. The evolution of the CSH coat with temperature can be clearly seen. At 25°C temperature, CSH products appear as winded slight sheets. At 150°C, the material presents a large network of cracks; one of them is visible in Figure 7-b.

The appearance of cracks can be explained by water thermal dilation that induces the separation of the CSH sheets. This separation leads to the diminution of their mutual attraction forces. The weakening of the links between the hydrates can initiate micro-defects that can facilitate sliding (a decrease of the material resistance can be observed at this temperature). At a temperature of 300°C (Fig.

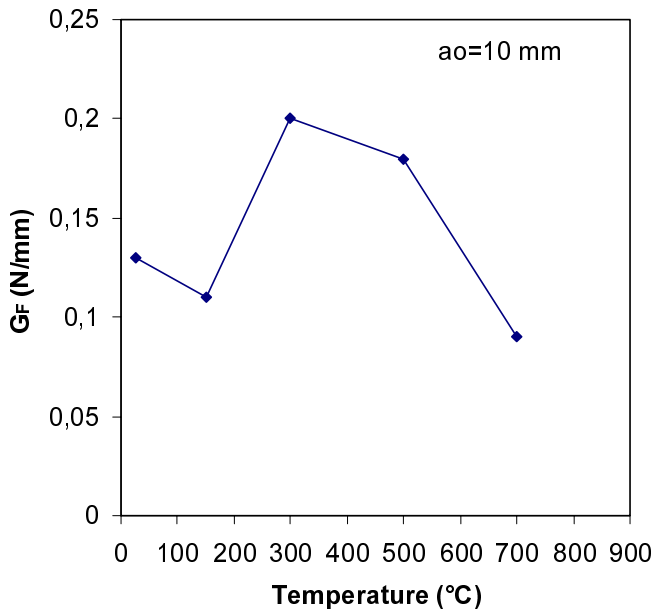


Figure 6. Variation of the fracture energy of the 10 mm length notched specimens vs. testing temperature.

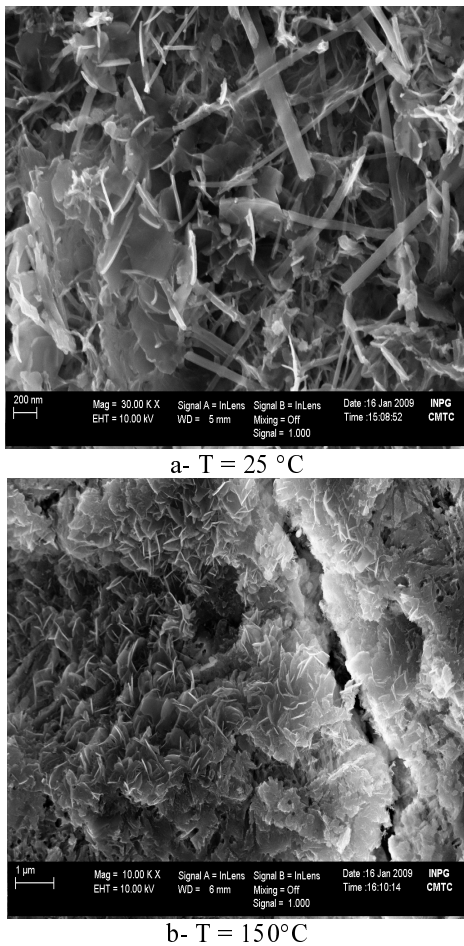


Figure 7. SEM micrographs of mortar at various testing temperatures. Hydrates are abundant at 25°C and 150°C, but cracks appear at 150°C.

8-a), the morphology becomes more compact and the CSH becomes corded. Close attention to the micrographs at this temperature reveals that the micro-cracks that appeared at 150°C are bridged by the CSH transform products; this phenomenon clearly explains the material resistance increase at

300°C. The CSH transformation is probably due to material dehydration which connects previously separated sheets.

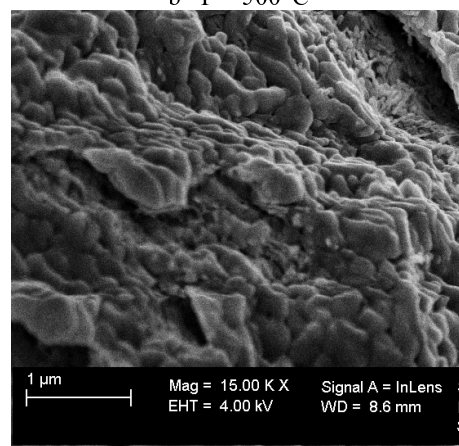
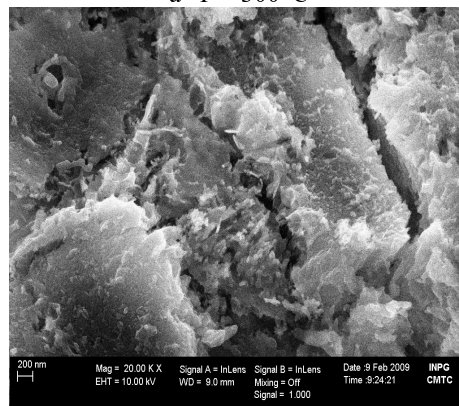
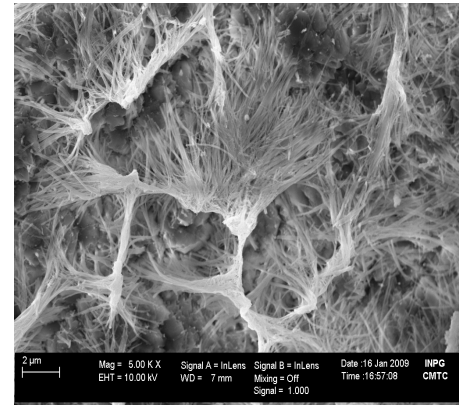


Figure 8. SEM micrographs of the investigated mortar when subjected to a- 300°C, b-500°C and c- 700°C testing temperatures. Whereas hydrates (CSH) are present at 300 and 500°C, such phases are no more visible at 700°C.

At 500°C (Fig. 8-b), the material exhibits regular micro-cracking. The CSH have dehydrated but are still slightly present, and the Portlandite phase began its decomposition. But at 700°C (Fig. 8-c), the CSH products are no longer visible and have been replaced by CS or CS₂ phase structures. The transformation and subsequent disappearance of the CSH coat at temperatures of 700°C and higher are accompanied by a drastic reduction in the material resistance (Fig. 3).

A synthesis of the SEM micrographs analysis and

a chemical analysis (not presented here) revealed that the evolution of the mortar mechanical properties with temperature is correlated to microstructure evolution, water loss, and dehydration reactions. Chemical decomposition using x-ray analysis or thermogravimetric analysis (TGA) should also confirm our results; these investigations will be undertaken later. This material should be further tested at this particular temperature. Lastly, the investigated material is more similar to mortar than concrete. Thus, unlike concrete, the propagation of the initiated cracks is unlikely to be stopped by the presence of a grain.

4 CONCLUSIONS

The aim of the present work is to investigate high performance concrete mortar behaviour when subjected to increasing testing temperatures. A three-point bending test apparatus was developed in alumina material, and tests were conducted by loading 10 mm length notched specimens that had been heated to various temperatures (25, 150, 300, 500, 700, and 900°C).

- Below a temperature of 500°C the material exhibited nonlinear quasi-brittle behaviour with good resistance. At temperatures up to 700°C, the behaviour changed to nonlinear with pseudo-ductility and notably lesser resistance. The optimal resistance is obtained within the 300-500°C temperature range, and the material exhibits no resistance at 900°C.

- The tenacity parameters, including the stress intensity factor K_I and the fracture energy G_F , have been determined. Their evolution with temperature behaves in a similar fashion as the peak load vs. temperature.

- An analysis of SEM micrographs showed that cracks first occur at a temperature of 150°C with a decreasing peak load. A bridging phenomenon for these cracks at 300°C was then observed, accompanied by CSH transformations and an increase of the peak load. As the temperature further increased, the hydrate products evolved as a new micro-cracking phenomenon appeared at 500°C. Finally, the disappearance of hydrates at temperatures over 700°C was accompanied by a drastic decrease in material resistance. The microstructure observations were consistent with the macroscopic thermo-mechanical behaviour of the material, as determined by the three-point bending tests. Analysis of the hydrates evolution has been proposed.

REFERENCES

Bazant, Z.P. & Kazemi, M.T. 1990. Determination of fracture energy, process zone length and brittleness number from size effect, with application to rock and concrete. *International Journal of Fracture* 44: 111-113.

Chan, Y.N., Luo X., Sun, W., 2000, Effects of high temperatures and cooling regimes on the compressive strength and the pore properties of high performance concrete, *Constructions and Building Materials*, 14 (2000) 261-266.

Chan, Y.N., Luo X., Sun, W., 2000, Compressive strength and pore structures of high-performance concrete after exposure to high temperature up to 800°C, *Cement and Concrete Research* 30 (2000) 247-251.

Diamond, S. 1986. The Microstructure of Cement Paste in Concrete, *VIII International Cong. Chem. Cem, Rio de Janeiro 1986* 1: 113-121.

Diederichs, U., Jumpanem, U.-M. & Penttala, V. 1988. Material properties of high strength concrete at elevated temperature, *IABSE 13th Congress*, Helsinki, 1988.

Fellegetti, R., Gambarova, P.G., Rosati, G.P., Corsi, F. & Giannuzzi, G. 1996. Residual Mechanical properties of high strength Concretes Subjected to High Temperature Cycles. *Proc. of 4th International Symposium on Utilization of High Strength/High Performance Concrete, Paris, France 1996*, 579-588.

GjØrv, O.E., Sorensen, S.F. & Arnesen, A. 1977. Notch sensitivity and fracture toughness of concrete, *Cement and concrete Research*, 7: 333-344.

Hillerborg, A. & Petersson, P.E. 1980. Fracture mechanical calculations. Test methods and results for concrete and similar materials. *Proceedings of the 5th International Conference on Fracture, Cannes, 1980*.

Kaplan, M.F. 1961. Crack propagation and the fracture of concrete, *A.C.I. Journal*, 58 (5): 591-610.

Khoury, G.A., Grainger, B.N. & Sullivan, G.P.E. 1985. Strain of concrete during first heating to 600°C under load. *Magazine of Concrete Research*, 37: 195-215.

Menou, A., Mounajed, G., Boussa, H., Pineaud, A., Carre, H., residual fracture energy of cement paste, mortar and concrete subject to high temperature, *Theoretical and Applied Fracture Mechanics* 45 (2006) 64-71.

Noumowe, A., Clasteres, P., Debicki, G. & Bolvin, M., 1994. High temperature Effects of High Performance Concrete: Strength and porosity. *Third CANMET/ACI International Conference on Durability of Concrete, Nice, France, 24-28 May, 1994*.

RILEM 50-FMC on fracture Mechanics of concrete, 1985. Determination of fracture Energy of Mortar and Concrete by means of three-Point bending tests on notched Beams, *Materials and Structures* 18(106): 285-290.

RILEM TC 129-MHT 2000, Test methods for mechanical properties of concrete at high temperatures Recommendations, Part8-Steady-state creep and creep recovery for service and accident conditions. *Materials and Structures* 33: 6-13.

Schrefler, B.A.F.E., 1995. Coupled thermo-hydro-mechanical processes in porous media including pollutant transport, *Archives of Computational Methods in Engineering*, in *Environmental Engineering* 2(3): 1-1. by CIMM, Barcelona - Spain.

Swamy, R.N. 1983. Linear elastic fracture mechanics parameters of concrete, *Fracture mechanics of concrete*, Ed, F.H. Wittman, Editor, *Fracture Mechanics of Concrete*, Elsevier Sciences Publishers, Netherlands (1983), pp. 411-461.

Ziegeldorf, S. 1983. Fracture mechanics parameters of hardened cement paste, aggregates and interfaces, *Fracture Mechanics of Concrete*, Ed. F.H. Wittman, Editor, *Fracture Mechanics of Concrete*, Elsevier Sciences Publishers, Netherlands (1983), pp. 371-409.